Domain IV voltage-sensor movement is both sufficient and rate limiting for fast inactivation in sodium channels

Deborah L. Capes,[1] Marcel P. Goldschen-Ohm,[1] Manoel Arcisio-Miranda,[1] Francisco Bezanilla,[2] and Baron Chanda[1]

[1]Department of Neuroscience, University of Wisconsin, Madison, Madison, WI 53706
[2]Department of Biochemistry and Molecular Biology, University of Chicago, Chicago, IL 60637

Voltage-gated sodium channels are critical for the generation and propagation of electrical signals in most excitable cells. Activation of Na^+ channels initiates an action potential, and fast inactivation facilitates repolarization of the membrane by the outward K^+ current. Fast inactivation is also the main determinant of the refractory period between successive electrical impulses. Although the voltage sensor of domain IV (DIV) has been implicated in fast inactivation, it remains unclear whether the activation of DIV alone is sufficient for fast inactivation to occur. Here, we functionally neutralize each specific voltage sensor by mutating several critical arginines in the S4 segment to glutamines. We assess the individual role of each voltage-sensing domain in the voltage dependence and kinetics of fast inactivation upon its specific inhibition. We show that movement of the DIV voltage sensor is the rate-limiting step for both development and recovery from fast inactivation. Our data suggest that activation of the DIV voltage sensor alone is sufficient for fast inactivation to occur, and that activation of DIV before channel opening is the molecular mechanism for closed-state inactivation. We propose a kinetic model of sodium channel gating that can account for our major findings over a wide voltage range by postulating that DIV movement is both necessary and sufficient for fast inactivation.

The Journal of General Physiology

INTRODUCTION

Voltage-gated sodium channels are responsible for the initiation of action potentials in excitable tissues including heart, brain, and skeletal muscle (Hodgkin and Huxley, 1952). Channel activation involves conformational changes in four voltage sensors that surround a central ion-conducting pore (Catterall, 2010). Sodium channels also rapidly inactivate via an occlusion of the pore by an intracellular hydrophobic motif (West et al., 1992; Eaholtz et al., 1994), which helps reset the membrane to its resting condition. Inherited mutations that disrupt inactivation are associated with serious human diseases including muscular dysfunction (Cannon, 1996; Hayward et al., 1996; Jurkat-Rott et al., 2010), epilepsy (Wallace et al., 1998), and cardiac arrhythmias such as long QT syndrome (Wang et al., 1995a,b, 1996; Ackerman, 1998; Kambouris et al., 1998). Despite their physiological importance, far more is known about the structurally similar voltage-gated potassium channel. However, whereas potassium channels are comprised of four identical subunits, sodium channels have four homologous but non-identical domains, DI–IV (Bezanilla, 2000). This asymmetry gives rise to distinct functional roles for specific domains.

Mutagenesis studies have shown that perturbations in specific voltage sensors have differential effects on channel function, with mutations in voltage sensor of domain IV (DIV) primarily affecting inactivation (Chahine et al., 1994; Yang and Horn, 1995; Chen et al., 1996; Lerche et al., 1997; McPhee et al., 1998; Kühn and Greeff, 1999; Sheets et al., 1999). Monitoring the movement of individual voltage sensors with site-specific fluorescent probes subsequently revealed that DI–III activate with similar kinetics to those of current rise, whereas DIV moves relatively slower with a time course that tracks current inactivation (Chanda and Bezanilla, 2002). Consistent with a preferential role of DIV in inactivation, toxins that inhibit movement of the DIV voltage sensor destabilize fast inactivated state(s), whereas toxins that bind to DI–III voltage sensors largely affect channel activation (Hanck and Sheets, 2007; Bosmans et al., 2008).

Although the above studies implicate inactivation as primarily involving the DIV voltage sensor, mutations in other domains including disease mutants throughout

D.L. Capes, M.P. Goldschen-Ohm and M. Arcisio-Miranda contributed equally to this paper.
Correspondence to Baron Chanda: chanda@wisc.edu
D.L. Capes's present address is Dept. of Neurobiology, Harvard Medical School, Boston, MA 02115.
M. Arcisio-Miranda's present address is Dept. of Biophysics, University of São Paulo, 05508-070 São Paulo, Brazil.
Abbreviations used in this paper: CTX, μ-conotoxin; DIV, voltage sensor of domain IV.

The Rockefeller University Press $30.00
J. Gen. Physiol. Vol. 142 No. 2 101–112
www.jgp.org/cgi/doi/10.1085/jgp.201310998

the channel can affect macroscopic inactivation (Kontis and Goldin, 1997; Jurkat-Rott et al., 2000, 2010). For example, disruption of inactivation by a mutation in the DIII S4–S5 linker can be partially rescued by an opposite charge swap in the inactivation motif, suggesting that both DIII and DIV contribute to the docking site for the inactivation motif (Lerche et al., 1997; Smith and Goldin, 1997; McPhee et al., 1998). Also, development of fast inactivation is correlated with immobilization of the gating charge in DIII and DIV (a slowing of the gating charge return upon repolarization) (Armstrong and Bezanilla, 1977; Cha et al., 1999). However, it remains unclear whether charge immobilization reflects a tight coupling between the DIII/IV voltage sensors and fast inactivation, or simply an intrinsic property of the voltage sensors themselves (Sheets et al., 2000; Bosmans et al., 2008). Thus, the detailed role of each individual voltage sensor in fast inactivation, including which voltage sensors or combinations of voltage sensors, if any, are either required or are sufficient for inactivation, remains unclear.

Here, we functionally impaired each individual voltage sensor one at a time by neutralizing the first three arginines in their S4 segments via mutation to glutamine. These arginines have been shown previously to contribute most of the gating charge (Sheets et al., 1999). Similar voltage-sensor neutralizations in potassium channels result in a voltage-independent stabilization of the affected sensor in its activated state (Bao et al., 1999; Gagnon and Bezanilla, 2009). Thus, we hypothesized that neutralization of the critical gating charges in an individual voltage sensor of the sodium channel would allow us to study the properties of fast inactivation in the absence of that particular source of voltage dependence. Here, we show that the rate-limiting step to both development and recovery from fast inactivation is movement of the DIV voltage sensor, of which the activation is alone sufficient for inactivation to occur. Our data suggest that DIV movement before pore opening is the molecular basis for fast inactivation from closed states. We propose a kinetic model that can explain our kinetic observations for entry and recovery from inactivation over a wide voltage range, as well as the effect of charge neutralizations in DIV, by postulating that activation of DIV is both necessary and sufficient for fast inactivation.

MATERIALS AND METHODS

Molecular biology

Each construct was generated by serial mutagenesis of each of the three gating charges in a specific domain to glutamine using a QuikChange mutagenesis kit (QIAGEN). Mutations were verified by sequencing of the entire coding region. Each construct was cloned into a pBSTA vector previously optimized for expression in oocytes (Chanda and Bezanilla, 2002). For injection in oocytes, cRNA was transcribed from the cDNA using a T7 RNA polymerase kit (Applied Biosystems).

Heterologous expression in *Xenopus laevis* oocytes

Oocytes were extracted surgically from *Xenopus* and the follicular layer was removed using a combination of mechanical separation and 30–60 min of treatment with 1 mg/ml collagenase A. Oocytes were subsequently stored at 18°C in a solution containing (mM): 100 NaCl, 2 KCl, 1.8 $CaCl_2$, 1 $MgCl_2$, and 5 HEPES, pH 7.2, which was further supplemented with 100 µM DTT, 0.2 mM EDTA, and 100 µg/ml gentamicin (Invitrogen). Oocytes were coinjected with the α subunit of one of the rat Nav1.4 constructs along with the associated β_1 subunit in a 1:1 molar ratio (50 ng α subunit to 10 ng β_1 subunit per oocyte) using a microinjector (Nanoliter 2000; World Precision Instruments).

Electrophysiology

Recordings were performed either with a two-electrode voltage clamp (OC-725C Oocyte Clamp; Warner Instruments) or a modified cut-open oocyte setup as we have described previously (Muroi et al., 2010). For all experiments, the intracellular solution contained (mM): 105 *N*-methyl-D-glucamine (NMG), 20 HEPES, and 2 EGTA, pH 7.4 with methanesulfonic acid (MES). For ionic current measurements, the extracellular solution contained (mM): 105 NaMES, 20 HEPES, and 2 $Ca(OH)_2$, pH 7.4 with MES. For

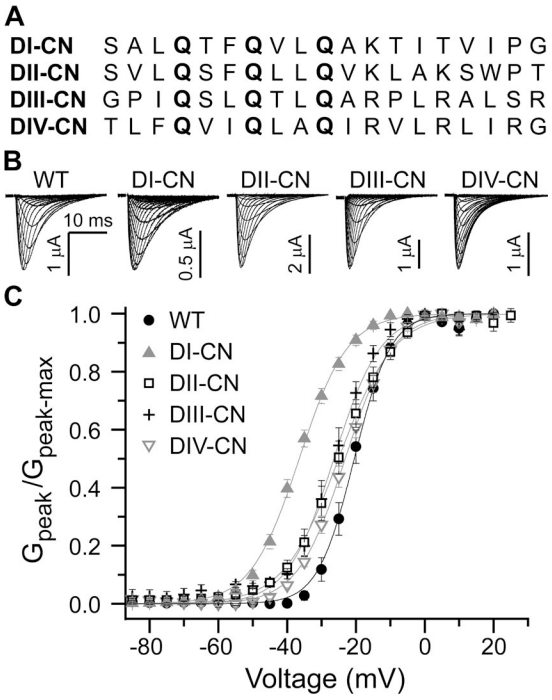

Figure 1. Domain-specific charge neutralizations. (A) Sequence alignments of the S4 voltage-sensing segments from each domain in Nav1.4. Mutations are marked in bold. (B) A representative family of ionic current traces for wild-type and mutant channels in response to 30-ms depolarizing pulses from −110 to 65 mV (10-mV steps), preceded by a 20-ms prepulse to −120 mV from a holding potential of −80 mV. (C) Normalized peak G-V relationship for wild-type and mutant channels. Solid lines are single Boltzmann fits to the mean for each construct (wild type: $V_{1/2}$ = −23.8 mV and z = 5.8 e^-; DI-CN: $V_{1/2}$ = −36.5 mV and z = 3.8 e^-; DII-CN: $V_{1/2}$ = −25.1 mV and z = 3.3 e^-; DIII-CN: $V_{1/2}$ = −26.4 mV and z = 3.9 e^-; DIV-CN: $V_{1/2}$ = −23.1 mV and z = 3.8 e^-).

gating current recordings, the extracellular solution contained (mM): 105 NMG-MES, 20 HEPES, and 2 $Ca(OH)_2$, pH 7.4 with MES. For the gating current recordings, μ-conotoxin (CTX) was added to the external solution at concentrations ranging from 6 to 25.7 μM to block currents through the pore.

Data acquisition and analysis

Recordings were acquired at 250 kHz using a digitizer (Axon Digidata 1440; Molecular Devices) and amplifier (CA-1B; Dagan) with pCLAMP software (Molecular Devices). Analysis was performed in pCLAMP 10 (Molecular Devices) and Excel (Microsoft). Bi-exponential fits with a variable lag to onset for both development and recovery from inactivation were obtained using custom scripts in MATLAB (The MathWorks, Inc.). Boltzmann fits to conductance–voltage relations were performed in Origin (OriginLab).

Kinetic modeling

Kinetic modeling was performed with custom routines written in C++. The time-dependent probability in each state of the model was solved numerically from the matrix of transition rates as described by Colquhoun and Hawkes (1995). Rate constants were optimized by minimizing the sum of squared errors between observed and simulated data using a simplex algorithm.

RESULTS

Neutralization of the first three gating charges in individual voltage sensors

We generated four mutants in which the first three arginine residues comprising the majority of the gating charge in a specific voltage sensor were neutralized via mutation to glutamine. Hereafter, we refer to these charge-neutralization mutants as DI-CN, DII-CN, DIII-CN, and DIV-CN, where, for example, DIV-CN represents the mutant with three charge neutralizations in DIV (Fig. 1 A). All of the mutants were functional with current kinetics that were not grossly different than wild type in response to 30-ms depolarizing voltage steps from −100 to 65 mV, 10-mV steps (Fig. 1 B). Each depolarization was preceded by a 50-ms prepulse to −120 mV from a holding potential of −80 mV, except for DIV-CN, which was preceded by a prepulse to −180 mV, as this mutant was largely inactivated at −120 mV (see below). Each mutant exhibited a G-V curve that was slightly left-shifted as compared with wild type (Fig. 1 C).

DIV voltage-sensor movement is sufficient for fast inactivation

Steady-state inactivation during a 100-ms conditioning voltage pulse from −170 to 50 mV was assayed with a subsequent 30-ms test pulse to −30 mV to assess the fraction of noninactivated channels. The conditioning pulse was preceded by a 20-ms prepulse to −120 mV, and a 1-ms pulse to −120 mV separated each conditioning/test pulse pair to close noninactivated channels before the test pulse. DI-CN, DII-CN, and DIII-CN had no effect on the voltage dependence of steady-state inactivation as compared with wild type, whereas DIV-CN channels were largely inactivated at potentials as hyperpolarized as −120 mV (Fig. 2, A and B). However, the DIV-CN steady-state inactivation versus voltage relation did not saturate above −200 mV, and thus the reported median voltage for this mutant is an upper limit, where the actual value may be quite a bit more hyperpolarized. Therefore, neutralization of the gating charges in the DIV voltage sensor allows fast inactivation to occur at voltages much more hyperpolarized than is usual, whereas neutralization of gating charges in DI–III has little effect on steady-state inactivation. Because it is unlikely that voltage sensors with intact gating charges will be activated at hyperpolarized potentials such as −120 mV, these data suggest that activation of DIV alone is sufficient for fast inactivation to occur.

DIV voltage-sensor movement is rate limiting for development of fast inactivation

We hypothesized that neutralizing the critical gating charges in a specific voltage sensor would reduce the voltage dependence and speed the rate of development of fast inactivation only if that voltage sensor were involved in formation of fast inactivated state(s). To test

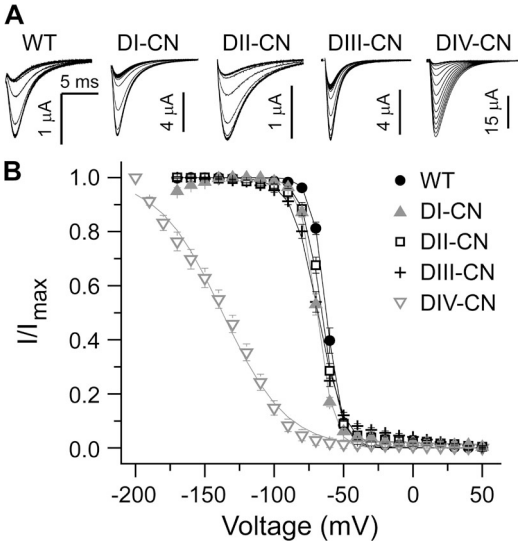

Figure 2. DIV voltage-sensor movement is sufficient for fast inactivation. (A) A representative family of current traces in response to a 30-ms test pulse to −30 mV to assay the fraction of non–steady-state inactivated channels after a 100-ms conditioning prepulse between −170 and 50 mV. See Results for a detailed description of the voltage-pulse protocol. (B) Normalized steady-state inactivation versus conditioning prepulse voltage for wild-type and mutant channels. Solid lines are single Boltzmann fits to the mean for each construct (wild type: $V_{1/2}$ = −62.3 mV and z = 4.7 e^-; DI-CN: $V_{1/2}$ = −69.2 mV and z = 4.2 e^-; DII-CN: $V_{1/2}$ = −65.8 mV and z = 3.7 e^-; DIII-CN: $V_{1/2}$ = −68.7 mV and z = 2.7 e^-; DIV-CN: $V_{1/2}$ = −137.3 mV and z = 1.1 e^-). Note that the relation does not saturate above −200 mV for DIV-CN, so the observed left-shift in the steady-state inactivation versus voltage relation reflects the minimum shift conferred by this mutant.

this, we measured the kinetics of development of fast inactivation over a wide voltage range for both wild-type and mutant channels. The time course of entry into fast inactivation was determined by assaying the fraction of noninactivated channels at the end of a variable length conditioning pulse (0.1–50 ms) with a 30-ms test pulse to 0 mV (Fig. 3 A). The conditioning pulse was preceded by a 20-ms prepulse to −120 mV, and a 1-ms pulse to −100 mV separated each conditioning/test pulse pair to close noninactivated channels before the test pulse. The rate of development of fast inactivation at different voltages was assayed with conditioning pulses ranging from −120 to 0 mV (Fig. 3 B).

For wild-type channels, there is a characteristic lag after the onset of a depolarization preceding entry into fast inactivation. This lag is voltage dependent, decreasing with increasing depolarization, and reflected as a sigmoidal foot in the time course of development of fast inactivation plotted in Fig. 3 B. For each voltage, the time course of entry into fast inactivation was fit with a double-exponential rise whose onset was allowed to lag time zero (Fig. 3, C and D). As compared with wild

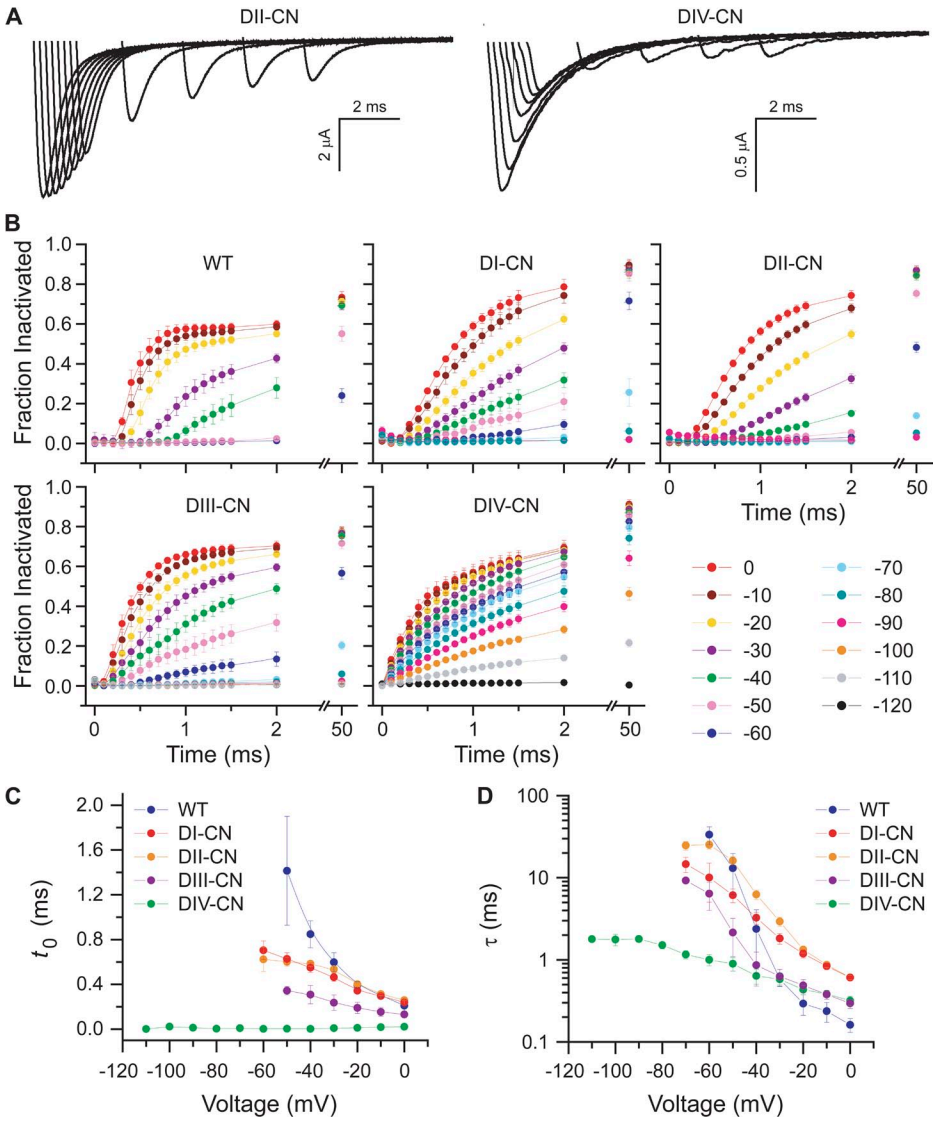

Figure 3. DIV voltage-sensor movement is rate limiting for development of fast inactivation. (A) Representative families of traces illustrating current responses to a 0-mV test pulse after development of inactivation during a variable duration conditioning pulse at −30 mV. See Results for a detailed description of the voltage-pulse protocol. (B) Summary of the time course of development of fast inactivation for conditioning voltages spanning −120 to 0 mV. (C and D) For each conditioning voltage, the time course of development of fast inactivation shown in B was fit to the bi-exponential rise $\left\{A_1(1-e^{-(t-t_0)/\tau_1})+A_2(1-e^{-(t-t_0)/\tau_2})\right\}H(t-t_0)$, where t is the duration of the conditioning pulse, A_i and τ_i are the amplitudes and time constants of the rise (i = 1,2), H is the unit step function, and t_0 is the delay after onset of the conditioning pulse to initiation of development of fast inactivation. The voltage dependence of the delay and fast time constant for each construct is summarized in C and D, respectively (mean ± SEM).

type, the lag as well as its voltage dependence is largely maintained in the DI-CN and DII-CN mutants, slightly shortened for DIII-CN, and virtually eliminated at all voltages tested for DIV-CN (Fig. 3 C). Also, DIV-CN both slowed the fast time constant for development of inactivation and significantly reduced its voltage dependence, whereas the other mutants had little effect on either the kinetics or voltage dependence of entry into fast inactivation (Fig. 3 D). Collectively, these results suggest that formation of the fast inactivated state(s) involves primarily domains III and IV, and that DIV is both rate limiting and contributes most of the voltage dependence of development of fast inactivation.

DIV voltage-sensor movement is rate limiting for recovery from fast inactivation

Analogous to development of inactivation, we hypothesized that biasing a specific voltage sensor toward its activated conformation by neutralizing its critical gating charges would slow the rate of recovery from fast inactivation only if that voltage sensor were involved in recovery from fast inactivated state(s). To test this, we measured the kinetics of recovery from fast inactivation over a wide voltage range for both wild-type and mutant channels. The time course of recovery from fast inactivation was determined after a 30-ms inactivating pulse at −20 mV by assaying the fraction of noninactivated

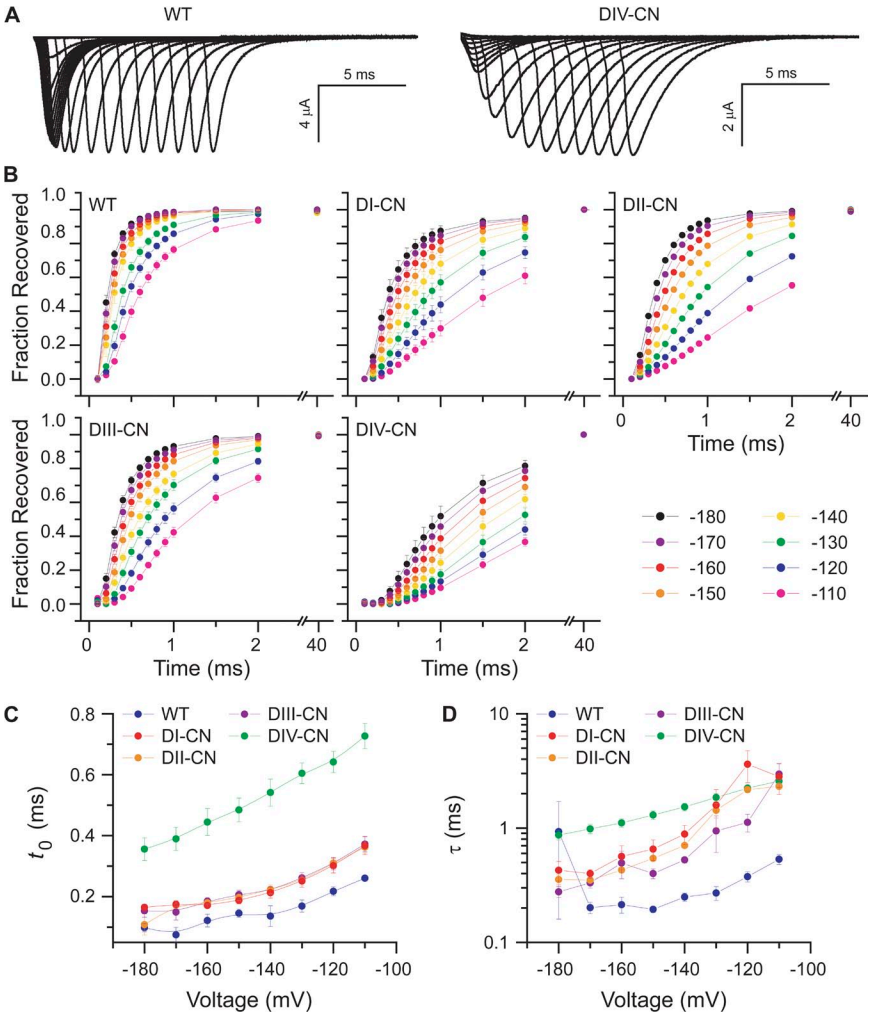

Figure 4. DIV voltage-sensor movement is rate limiting for recovery from fast inactivation. (A) Representative families of traces illustrating current responses to a −20-mV test pulse after recovery from inactivation during a variable duration conditioning pulse at −140 mV after initially inactivating the channels for 30 ms at −20 mV. See Results for a detailed description of the voltage-pulse protocol. (B) Summary of the time course of recovery from fast inactivation for conditioning voltages spanning −180 to −110 mV. (C and D) For each conditioning voltage, the time course of recovery from fast inactivation shown in B was fit to the bi-exponential rise $\left\{A_1(1-e^{-(t-t_0)/\tau_1})+A_2(1-e^{-(t-t_0)/\tau_2})\right\}H(t-t_0)$, where t is the duration of the conditioning pulse, A_i and τ_i are the amplitudes and time constants of the rise (i = 1,2), H is the unit step function, and t_0 is the delay after onset of the conditioning pulse to initiation of recovery from fast inactivation. The voltage dependence of the delay and fast time constant for each construct is summarized in C and D, respectively (mean ± SEM).

channels at the end of a variable-length hyperpolarized recovery pulse (0.1–40 ms) with a 30-ms test pulse to −20 mV (Fig. 4 A). The inactivating pulse was preceded by a 20-ms prepulse to −120 mV. The rate of recovery from fast inactivation at different voltages was assayed with recovery pulses ranging from −180 to −110 mV (Fig. 4 B).

For each voltage, the time course of recovery from fast inactivation was fit with a double-exponential rise (a single exponential was used for DIV-CN) whose onset was allowed to lag time zero as described above for development of inactivation (Fig. 4, C and D). In wild-type channels, the lag to recovery was quite short, with channels recovering almost immediately upon repolarization. In contrast, DIV-CN channels exhibited a pronounced lag with no recovery for almost 0.5 ms (Fig. 4 C). As compared with wild type, all of the mutants slowed recovery to some extent, although DIV-CN had the largest effect (Fig. 4 D). These data suggest that although each domain contributes somewhat, the return of the DIV voltage sensor is the rate-limiting step during recovery from fast inactivation.

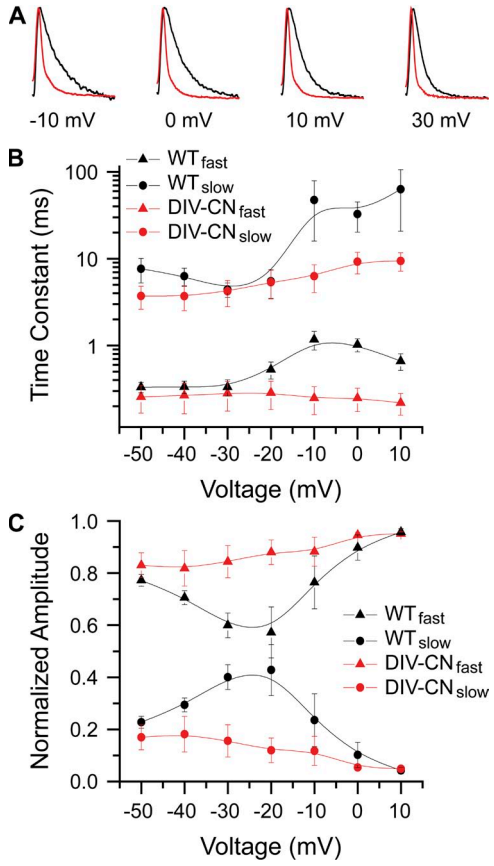

Figure 5. DIV-CN eliminates most of the gating charge movement associated with DIV. (A) Comparison of normalized ON gating currents for wild-type (black) and DIV-CN (red) channels in response to depolarizing voltage steps to −30, −10, and 0 mV after a 50-ms prepulse to −130 mV. Pore currents were blocked with CTX, which we have recently shown does not affect DIV gating charge movement, unlike tetrodotoxin (Capes et al., 2012). (B and C) ON gating currents were fit with a bi-exponential decay. The voltage dependence of the fast and slow time constants and their relative amplitudes for wild-type and DIV-CN channels is summarized in B and C, respectively (mean ± SEM; $n \geq 4$).

DIV-CN eliminates most of the gating charge movement associated with DIV

We hypothesized that if charge neutralizations in specific voltage sensors were to effectively immobilize them in their activated conformation, then their contribution to the gating currents should be eliminated. Because domains I, II, and III all contribute significantly to the fast component of gating charge movement, it is difficult to determine the effect of neutralization of any one of them (Chanda and Bezanilla, 2002). However, the slow component of ON gating currents has been largely attributed to movement of the DIV voltage sensor, which we predict should be mostly abolished in DIV-CN channels (Cha et al., 1999; Chanda and Bezanilla, 2002). To determine the contribution of the DIV voltage sensor to gating currents during channel activation, we compared ON gating currents for wild-type and DIV-CN channels. Because tetrodotoxin modifies the movement of DIV voltage sensor, we measured gating currents in the presence of the pore blocker CTX, which we have recently shown does not alter DIV gating currents (Capes et al., 2012).

As compared with wild type, most of the slow component in the DIV-CN ON gating currents is absent (Fig. 5, A and B). Double-exponential fits to ON gating current decay for wild-type and DIV-CN channels are summarized in Fig. 5 (C and D). The fast and slow time constants were similar for wild-type and DIV-CN channels. However, the amplitude of the slow component was greatly reduced for DIV-CN (maximum contribution of ∼18%) as compared with wild type. These results suggest that movement of the DIV voltage sensor is severely impaired in DIV-CN channels. We predict that movement of the other domains is similarly hampered by their respective charge neutralizations.

A kinetic model describing the distinct role of DIV in fast inactivation

To explain our above observations, we constructed a kinetic model of sodium channel gating where activation of the DIV voltage sensor is both necessary and sufficient for fast inactivation to occur (Fig. 6 A). In the model shown in Fig. 6 A, the horizontal transitions from left to right reflect activation of the DI–III voltage sensors followed by pore opening, whereas the vertical transitions from bottom to top reflect activation of the DIV voltage sensor followed by occlusion of the pore by the fast inactivation motif. Pore opening was allowed to occur after activation of DI–III regardless of the conformation of DIV, consistent with observations that the

DI–III voltage sensors track current rise, whereas the DIV voltage sensor moves more slowly with a similar time course to current inactivation (Chanda and Bezanilla, 2002), and also reports that toxins specifically inhibiting activation of the DIV voltage sensor do not affect channel activation (Hanck and Sheets, 2007).

The transition rate constants and charges were initially set to values similar to those used to describe sodium channels in squid axons (Vandenberg and Bezanilla, 1991). Although squid axon and skeletal muscle sodium channels differ somewhat in their behavior, this earlier model was constrained by both single-channel records and gating currents and thus represents a good starting point for the model developed here. As observed by Vandenberg and Bezanilla (1991), we treated movement of DI–III with three sequential identical transitions, consistent with positive cooperativity between voltage sensors. We further postulated that activation of DI–III allosterically biases activation of DIV as well as binding of the inactivation motif, similar to the effect of voltage-sensor activation on inactivation as described by Kuo and Bean (1994).

The model in Fig. 6 A qualitatively describes the detailed kinetics and voltage dependence of fast inactivation for both wild-type and each of the mutant channels over a wide voltage range. To account for the effects of the DIV-CN mutant, we modified the transition rates associated with movement of the DIV voltage sensor only (α_4/β_4) by reducing their charge and allowing their intrinsic rates to vary (they became slower), whereas all other parameters were constrained to their wild-type values. Because the model in Fig. 6 A does not distinguish between DI–III, we chose to simulate the general effect of these domain mutants by modifying the middle

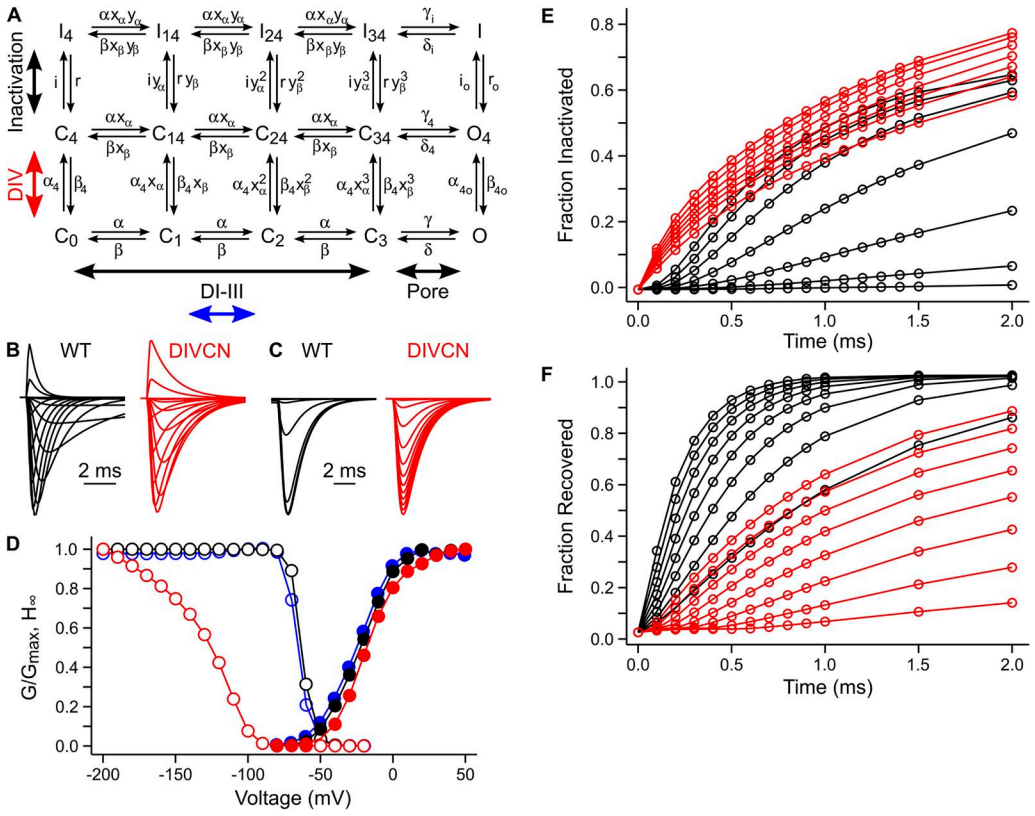

Figure 6. A sodium channel gating model for the distinct role of DIV in fast inactivation. (A) Kinetic model for sodium channel gating. The horizontal transitions from left to right reflect activation of the DI–III voltage sensors followed by pore opening, and the vertical transitions from bottom to top reflect activation of the DIV voltage sensor followed by occlusion of the pore by the fast inactivation motif. Rate constants and associated charges are listed in Table 1. The effects of the DIV-CN mutant were explained solely by reducing the charge and varying the rates associated with movement of the DIV voltage sensor only such that DIV was biased toward its activated conformation (red arrow; see Table 1 for parameter values). The effects of the DI/II/III-CN mutants were qualitatively explained by reducing the charge and varying the rates for only the middle set of transitions associated with movement of the DI–III voltage sensors (blue arrow; see Table 1 for parameter values). (B) Simulated current responses to families of depolarizing voltage steps as described for Fig. 1 B. (C) Simulated current responses to a steady-state inactivation protocol as described for Fig. 2 A. (D) Simulated peak conductance (closed circles) and steady-state inactivation (open circles) as a function of voltage for wild-type (black), DIV-CN (red), and DI/II/III-CN (blue) channels. (E and F) Simulated time courses for development (−60 to 0 mV) and recovery (−180 to −110 mV) from inactivation for wild-type (black) and DIV-CN (red) channels. Note that fraction inactivated/recovered was not computed as the direct probability of being in one of the model's inactivated states but rather was obtained from simulated current responses as described in Figs. 3 B and 4 B. Simulations for DI/II/III-CN channels were similar to wild type.

set of horizontal voltage-sensor transitions associated with movement of one of the DI–III voltage sensors by reducing their charge and allowing their rates to vary, as described for DIV-CN.

The model was optimized by simultaneously minimizing the sum of squared errors between simulated and observed G-V, steady-state inactivation versus voltage, and the kinetics of both development and recovery from inactivation across a wide range of voltages for both wild-type and DVI-CN channels. The optimized wild-type model was then refit to the same datasets for DII-CN channels as described above for a general example of the model's ability to explain the behavior of the DI–III mutants. The final rate constants are listed in Table 1. This model explains both the kinetics and voltage dependence of observed sodium channel currents (Fig. 6, B and D), as well as the left-shift of steady-state inactivation for DIV-CN but not DI/II/III-CN (Fig. 6, C and D). Primarily, the model in Fig. 6 A accounts for the voltage dependence and kinetics of both development and recovery from fast inactivation over a wide voltage range, and the effects of single domain charge neutralizations on this behavior (Fig. 6, E and F). In particular, this model not only describes the reduction in the lag to entry into inactivation but also the prolongation of the lag to recovery from inactivation upon neutralization of the critical gating charges in DIV.

DISCUSSION

To study the role of individual voltage sensors in fast inactivation, we neutralized the critical gating charges in specific voltage sensors to determine the effect of removing the voltage-dependent gating transitions associated with distinct voltage sensors on fast inactivation. We have shown previously that these charge neutralizations give rise to hyperpolarization-activated omega currents through the voltage sensors themselves, which implies that the mutated voltage sensors retain some voltage-sensitive charge (Capes et al., 2012). However, several lines of evidence suggest that they have been severely biased toward their activated conformations. First, neutralization of these charges in DIV nearly eliminated the slow component of ON gating currents associated with movement of DIV (Fig. 5) (Cha et al., 1999; Chanda and Bezanilla, 2002), suggesting that the mutated voltage sensor contributes very little to the total gating charge movement. Second, DIV-CN left-shifted the

TABLE 1

Kinetic model parameters

Rate constant	k_0	q	Cooperativity factor	Value
	s^{-1}	e^-		
α	14,910	0.32	x_α	1.0
β	800	−0.91	x_β	0.12
α_4	2,100	0.21	y_α	1.0
β_4	1.89×10^6	−2.39	y_β	0.86
α_{4o}	1,410	0.21		
β_{4o}	170	−2.39		
γ	14,640	1.99		
δ	700	−0.5		
δ_4	1,000	−0.5		
δ_i	1,000	−0.5		
i	24,880	0.01		
r	600	−0.3		
i_o	22,500	0.01		
r_o	1.6	−0.3		
DIV-CN α_4	520	0.01		
DIV-CN β_4	3,630	−0.01		
DIV-CN α_{4o}	750	0.01		
DIV-CN β_{4o}	1.5	−0.01		
DI/II/III-CN α[a]	9,550	0.01		
DI/II/III-CN β[a]	390	−0.01		

The rate constant k_0 and voltage-dependent charge q for each unique transition in the model shown in Fig. 6 A, where the final transition rate k at any given voltage is computed as $k = k_0 e^{-qV/k_BT}$, where V is voltage, k_B is Boltzmann's constant, and T is temperature. The factors x and y are constants reflecting the degree of cooperativity in the model between activation of the DI–III voltage sensors and activation of the DIV voltage sensor or binding of the fast inactivation motif, respectively. The charges associated with α_{4o}, β_{4o}, i_o, and r_o were constrained to be identical to those of α_4, β_4, i, and r, respectively. Similarly, the charges associated with γ_4, δ_4, γ_i, and δ_i were constrained to be identical to those of γ and δ. The rate constants for γ_4 and γ_i were constrained based on microscopic reversibility as $\gamma_4 = \delta_4\beta_4 x_\beta^3 \gamma\alpha_{4o} / \beta_{4o}\delta\alpha_4 x_\alpha^3$ and $\gamma_i = \delta_i r y_\beta^3 \gamma_4 i_o / r_o \delta_4 i y_\alpha^3$, in that order.

[a]DI/II/III-CN rates only apply to the middle set of horizontal transitions associated with DI–III voltage sensors.

steady-state inactivation curve by at least 75 mV, indicating that functional changes correlated with activation of DIV (Chanda and Bezanilla, 2002) are occurring at voltages where the voltage sensors would normally be at rest (Fig. 2). Finally, the voltage dependence of entry into inactivation was nearly eliminated for DIV-CN (Fig. 3, C and D), consistent with the idea that the relevant voltage-dependent conformational change in DIV has already occurred before the onset of an inactivating pulse. Although the effect of the charge neutralizations in DI–III on movement of each individual voltage sensor is harder to interpret, we hypothesize that they are biased toward their activated conformations in a similar fashion to DIV, and that the reduced functional effects of these mutants reflects the biasing of only one of three domains, of which the activation of all three is required for channel activation.

Channel activation

The left-shift in the G-V for each mutant is consistent with a role in activation for each of the four voltage sensors, where preactivating any one of them speeds activation by removing one of the voltage-dependent transitions in the activation pathway. However, shifts in the peak G-V are difficult to interpret in the presence of fast inactivation, which also contributes to shaping the peak current response and open probability (Aldrich et al., 1983; Goldschen-Ohm et al., 2013). Thus, a left shift in the peak G-V could also arise from faster inactivation (Gonoi and Hille, 1987). However, whereas DI-CN and DII-CN exhibited similarly minor effects on the voltage dependence and kinetics of development of fast inactivation, DI-CN conferred the largest hyperpolarizing shift in the peak G-V, suggesting that movement of the DI voltage sensor may be the rate-limiting step during channel activation.

Development of inactivation

DI-CN, DII-CN, and DIII-CN had no effect on steady-state inactivation, suggesting that activation of any one of these domains alone is not sufficient to promote fast inactivation. Consistent with this idea, none of these mutants had much of an effect on the voltage dependence or rate of entry into inactivation. However, DIII-CN did reduce the lag to entry into fast inactivation, suggesting that activation of DIII speeds inactivation but is alone not sufficient for fast inactivation to occur. In contrast, DIV-CN channels were largely steady-state inactivated at potentials where the channels were closed with the DI–III voltage sensors presumably held in their resting conformations by their intact gating charges. This implies that activation of DIV alone is sufficient for inactivation to occur, and suggests that closed-state inactivation during normal gating may reflect the allosteric activation of DIV before pore opening. DIV-CN also reduced the voltage dependence and eliminated the lag to development of fast inactivation, which further suggests that DIV is not only sufficient but also the rate-limiting step to formation of the fast inactivated state. These observations are consistent with our recent findings that DIV movement confers a conformational change in the pore necessary for rapid binding of the inactivation motif (Goldschen-Ohm et al., 2013).

Recovery from inactivation

In addition to slowing recovery from inactivation, DIV-CN introduced a prolonged lag before recovery. This suggests that movement of DIV is the rate-limiting step not only for development but also for recovery from fast inactivation. Consistent with this interpretation, toxins that inhibit activation of the DIV voltage sensor speed recovery from fast inactivated states and eliminate the lag preceding recovery onset (Richard Benzinger et al., 1999). All of the mutants slowed recovery from inactivation to some degree, although DIV-CN had the greatest effect. Thus, recovery from inactivation is most efficient when all of the voltage sensors are in their resting conformations. This suggests that each voltage sensor contributes to stabilization of fast inactivated state(s), with DI–II having the least influence and DIV having the most. This could be caused by coupling between domains, or it may reflect a second conformational change in individual voltage sensors, from which return during repolarization is impaired by fast inactivation, possibly by a steric hindrance from the bound fast inactivation motif (Kuo and Bean, 1994). These observations are consistent with reports that charge immobilization predominantly occurs for DIII–IV (Cha et al., 1999), but further imply that DI–II should undergo some small amount of immobilization as well.

Molecular determinant for closed-state inactivation

Wild-type sodium channels can fast inactivate before they open (Horn et al., 1981). Thus, most models of sodium channel gating include a transition not only from open to inactivated states but also from one or more closed states along the activation pathway to an inactivated state (Horn and Vandenberg, 1984; Vandenberg and Bezanilla, 1991; Kuo and Bean, 1994). DIV alone is sufficient to induce inactivation at potentials where the channel is predominantly closed, suggesting that activation of DIV before pore opening is the molecular basis of fast inactivation from closed states. Consistent with this idea, a comparison of the time course of entry into fast inactivation at −30 mV with the macroscopic kinetics of channel opening shows that whereas fast inactivation develops with a similar time course to current rise in wild-type channels, fast inactivation develops before current onset in DIV-CN channels (Fig. 7). The ability of DIV movement to account for inactivation from closed states is further explored in the kinetic model depicted in Fig. 6 A.

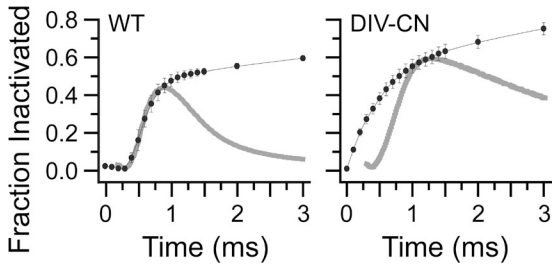

Figure 7. DIV voltage-sensor movement as a mechanism for fast inactivation from closed states. Representative current traces for wild-type and DIV-CN channels in response to a depolarization to −20 mV as shown in Fig. 1 B overlaid with their respective time courses for development of fast inactivation at −20 mV as shown in Fig. 3 B. Currents were scaled to the fraction of fast inactivated channels at the time of peak current. Development of fast inactivation precedes current rise for DIV-CN but not wild-type channels.

A sodium channel gating model

Our major findings that movement of the DIV voltage sensor is both sufficient and rate limiting for development and recovery from fast inactivation can be explained by the model in Fig. 6 A. This model postulates that DIV movement is not only sufficient but also necessary for fast inactivation to occur, and that the molecular basis for inactivation from closed states is activation of DIV before pore opening. In contrast to most sodium channel models that do not explicitly associate individual voltage-dependent transitions with specific voltage sensors (Horn and Vandenberg, 1984; Vandenberg and Bezanilla, 1991; Kuo and Bean, 1994), we explicitly treat DIV voltage-sensor movement as a separate allosteric transition from that of DI–III. Here, the return of DIV is the mechanism regulating the number of inactivated states that are traversed during recovery from inactivation, and thus the length of the lag preceding recovery (Fig. 4).

For the model in Fig. 6 A, we postulated that neutralization of the gating charges in DIV nearly abolishes the effective gating charge associated with this voltage sensor and slows its movement such that the DIV voltage sensor is biased toward its activated conformation. Consistent with our data, neutralizing the gating charges in DIV greatly reduces, but does not completely abolish, the voltage dependence of fast inactivation. The remaining voltage dependence for steady state, development, and recovery from fast inactivation in DIV-CN channels can be attributed to several mechanisms. First, the neutralized DIV in the model in Fig. 6 A is not completely locked in its activated conformation, such that activation of additional voltage sensors in DI–III contributes to stabilizing the activated DIV. Second, even when DIV is activated, there is an intrinsic voltage dependence associated with unbinding of the fast inactivation motif from its docking site in the pore, which we have estimated to involve ∼0.3 e^-, consistent with previous estimates from single-channel models that this step involves less than 1 e^- (Horn and Vandenberg, 1984; Vandenberg and Bezanilla, 1991).

The model in Fig. 6 A also explains why neutralizations in other domains have more limited effects on the kinetics of development and recovery from fast inactivation over a wide voltage range. Namely, preactivating any one of the DI, DII, or DIII voltage sensors has limited effects on activation and fast inactivation, as activation of the other two sensors becomes rate limiting. For example, reducing the charge and slowing the transition rates for one of the three horizontal transitions associated with movement of the DI–III voltage sensors had little effect on either the G-V or steady-state inactivation curves as observed for the DI/II/III-CN mutants (Fig. 6, C and D), and also exhibited kinetics for development and recovery from inactivation nearly identical to wild-type channels at all voltages tested. However, the model was not constrained to reproduce single-channel behavior or gating currents, and also does not account for the intermediate effects of DIII-CN between DI/II-CN and DIV-CN on the lag preceding both development and recovery from fast inactivation. Thus, more realistic models will need to explicitly treat each voltage sensor, as suggested by Chanda and Bezanilla (2002). However, constraining such a model remains a significant challenge because of a lack of domain-specific measurements (e.g., site-specific fluorescent probes) in combination with single-channel and gating current recordings in a single model system.

One sodium channel model that does explicitly treat both DIII and DIV voltage sensors was proposed by Armstrong (2006). Our model differs from that of Armstrong in that DIV voltage-sensor movement is not required for pore opening, consistent with observations that DIV movement can lag current rise (Chanda and Bezanilla, 2002), and that toxins inhibiting activation of DIV do not affect activation kinetics (Hanck and Sheets, 2007). DIV voltage-sensor movement in the model in Fig. 6 A gives rise to a second open-state preceding inactivation, consistent with recent observations based on multiple conductance levels in nonfast inactivating single channels (Goldschen-Ohm et al., 2013). For simplicity, both open states in this model were given an equal conductance, although setting the conductance of the second open state to two thirds that of the first, as we observed in the absence of fast inactivation, gave qualitatively similar results. However, it is possible that the DIV voltage sensor undergoes multiple conformational changes, some of which contribute to channel activation (Armstrong, 2006). Additionally, Armstrong (2006) postulates that inactivation from closed states requires activation of both DIII and DIV. In contrast, our data strongly suggest that movement of DIV alone is sufficient for fast inactivation to occur.

The model in Fig. 6 A provides a simple explanation for the detailed kinetics of development and recovery

from fast inactivation over a wide voltage range, as well as the predominant role of each individual voltage sensor in these processes. Specifically, this model accounts for our observations that movement of the DIV voltage sensor is both sufficient for fast inactivation to occur and also rate limiting for both development and recovery from fast inactivation. Furthermore, we propose that activation of the DIV voltage sensor before pore opening is the molecular basis for fast inactivation from closed states.

We thank Dr. Bob French for the gift of μ-conotoxin used for gating current studies.

This work was supported by research grants from National Institutes of Health (GM084140-01 to B. Chanda, GM30376 to F. Bezanilla, and T32-HL 07936 to D.L. Capes), a Shaw Scientist Award (to B. Chanda), and an American Heart Association (Midwest Affiliate) Postdoctoral Fellowship (12POST9440021 to M.P. Goldschen-Ohm).

Author Contributions: B. Chanda and F. Bezanilla conceived the study, and B. Chanda supervised the project. B. Chanda, D.L. Capes, and M. Arcisio-Miranda designed and performed the experiments. M.P. Goldschen-Ohm performed the kinetic modeling. M.P. Goldschen-Ohm, D.L. Capes, and B. Chanda wrote the manuscript.

Kenton J. Swartz served as editor.

Submitted: 1 April 2013
Accepted: 13 June 2013

REFERENCES

Ackerman, M.J. 1998. The long QT syndrome: ion channel diseases of the heart. *Mayo Clin. Proc.* 73:250–269. http://dx.doi.org/10.4065/73.3.250

Aldrich, R.W., D.P. Corey, and C.F. Stevens. 1983. A reinterpretation of mammalian sodium channel gating based on single channel recording. *Nature.* 306:436–441. http://dx.doi.org/10.1038/306436a0

Armstrong, C.M. 2006. Na channel inactivation from open and closed states. *Proc. Natl. Acad. Sci. USA.* 103:17991–17996. http://dx.doi.org/10.1073/pnas.0607603103

Armstrong, C.M., and F. Bezanilla. 1977. Inactivation of the sodium channel. II. Gating current experiments. *J. Gen. Physiol.* 70:567–590. http://dx.doi.org/10.1085/jgp.70.5.567

Bao, H., A. Hakeem, M. Henteleff, J.G. Starkus, and M.D. Rayner. 1999. Voltage-insensitive gating after charge-neutralizing mutations in the S4 segment of Shaker channels. *J. Gen. Physiol.* 113:139–151. http://dx.doi.org/10.1085/jgp.113.1.139

Bezanilla, F. 2000. The voltage sensor in voltage-dependent ion channels. *Physiol. Rev.* 80:555–592.

Bosmans, F., M.-F. Martin-Eauclaire, and K.J. Swartz. 2008. Deconstructing voltage sensor function and pharmacology in sodium channels. *Nature.* 456:202–208. http://dx.doi.org/10.1038/nature07473

Cannon, S.C. 1996. Sodium channel defects in myotonia and periodic paralysis. *Annu. Rev. Neurosci.* 19:141–164. http://dx.doi.org/10.1146/annurev.ne.19.030196.001041

Capes, D.L., M. Arcisio-Miranda, B.W. Jarecki, R.J. French, and B. Chanda. 2012. Gating transitions in the selectivity filter region of a sodium channel are coupled to the domain IV voltage sensor. *Proc. Natl. Acad. Sci. USA.* 109:2648–2653. http://dx.doi.org/10.1073/pnas.1115575109

Catterall, W.A. 2010. Ion channel voltage sensors: structure, function, and pathophysiology. *Neuron.* 67:915–928. http://dx.doi.org/10.1016/j.neuron.2010.08.021

Cha, A., P.C. Ruben, A.L. George Jr., E. Fujimoto, and F. Bezanilla. 1999. Voltage sensors in domains III and IV, but not I and II, are immobilized by Na+ channel fast inactivation. *Neuron.* 22:73–87. http://dx.doi.org/10.1016/S0896-6273(00)80680-7

Chahine, M., A.L. George Jr., M. Zhou, S. Ji, W. Sun, R.L. Barchi, and R. Horn. 1994. Sodium channel mutations in paramyotonia congenita uncouple inactivation from activation. *Neuron.* 12:281–294. http://dx.doi.org/10.1016/0896-6273(94)90271-2

Chanda, B., and F. Bezanilla. 2002. Tracking voltage-dependent conformational changes in skeletal muscle sodium channel during activation. *J. Gen. Physiol.* 120:629–645. http://dx.doi.org/10.1085/jgp.20028679

Chen, L.Q., V. Santarelli, R. Horn, and R.G. Kallen. 1996. A unique role for the S4 segment of domain 4 in the inactivation of sodium channels. *J. Gen. Physiol.* 108:549–556. http://dx.doi.org/10.1085/jgp.108.6.549

Colquhoun, D., and A.G. Hawkes. 1995. A Q-matrix cookbook. *In* Single-Channel Recording. B. Sakmann and E. Neher, editors. Plenum Press, New York. 589–633.

Eaholtz, G., T. Scheuer, and W.A. Catterall. 1994. Restoration of inactivation and block of open sodium channels by an inactivation gate peptide. *Neuron.* 12:1041–1048. http://dx.doi.org/10.1016/0896-6273(94)90312-3

Gagnon, D.G., and F. Bezanilla. 2009. A single charged voltage sensor is capable of gating the Shaker K^+ channel. *J. Gen. Physiol.* 133:467–483. http://dx.doi.org/10.1085/jgp.200810082

Goldschen-Ohm, M.P., D.L. Capes, K.M. Oelstrom, and B. Chanda. 2013. Multiple pore conformations driven by asynchronous movements of voltage sensors in a eukaryotic sodium channel. *Nat Commun.* 4:1350. http://dx.doi.org/10.1038/ncomms2356

Gonoi, T., and B. Hille. 1987. Gating of Na channels. Inactivation modifiers discriminate among models. *J. Gen. Physiol.* 89:253–274. http://dx.doi.org/10.1085/jgp.89.2.253

Hanck, D.A., and M.F. Sheets. 2007. Site-3 toxins and cardiac sodium channels. *Toxicon.* 49:181–193. http://dx.doi.org/10.1016/j.toxicon.2006.09.017

Hayward, L.J., R.H. Brown Jr., and S.C. Cannon. 1996. Inactivation defects caused by myotonia-associated mutations in the sodium channel III–IV linker. *J. Gen. Physiol.* 107:559–576. http://dx.doi.org/10.1085/jgp.107.5.559

Hodgkin, A.L., and A.F. Huxley. 1952. A quantitative description of membrane current and its application to conduction and excitation in nerve. *J. Physiol.* 117:500–544.

Horn, R., and C.A. Vandenberg. 1984. Statistical properties of single sodium channels. *J. Gen. Physiol.* 84:505–534. http://dx.doi.org/10.1085/jgp.84.4.505

Horn, R., J. Patlak, and C.F. Stevens. 1981. Sodium channels need not open before they inactivate. *Nature.* 291:426–427. http://dx.doi.org/10.1038/291426a0

Jurkat-Rott, K., N. Mitrovic, C. Hang, A. Kouzmekine, P. Iaizzo, J. Herzog, H. Lerche, S. Nicole, J. Vale-Santos, D. Chauveau, et al. 2000. Voltage-sensor sodium channel mutations cause hypokalemic periodic paralysis type 2 by enhanced inactivation and reduced current. *Proc. Natl. Acad. Sci. USA.* 97:9549–9554. http://dx.doi.org/10.1073/pnas.97.17.9549

Jurkat-Rott, K., B. Holzherr, M. Fauler, and F. Lehmann-Horn. 2010. Sodium channelopathies of skeletal muscle result from gain or loss of function. *Pflugers Arch.* 460:239–248. http://dx.doi.org/10.1007/s00424-010-0814-4

Kambouris, N.G., H.B. Nuss, D.C. Johns, G.F. Tomaselli, E. Marban, and J.R. Balser. 1998. Phenotypic characterization of a novel long-QT syndrome mutation (R1623Q) in the cardiac sodium

channel. *Circulation.* 97:640–644. http://dx.doi.org/10.1161/01.CIR.97.7.640

Kontis, K.J., and A.L. Goldin. 1997. Sodium channel inactivation is altered by substitution of voltage sensor positive charges. *J. Gen. Physiol.* 110:403–413. http://dx.doi.org/10.1085/jgp.110.4.403

Kühn, F.J., and N.G. Greeff. 1999. Movement of voltage sensor S4 in domain 4 is tightly coupled to sodium channel fast inactivation and gating charge immobilization. *J. Gen. Physiol.* 114:167–183. http://dx.doi.org/10.1085/jgp.114.2.167

Kuo, C.C., and B.P. Bean. 1994. Na+ channels must deactivate to recover from inactivation. *Neuron.* 12:819–829. http://dx.doi.org/10.1016/0896-6273(94)90335-2

Lerche, H., W. Peter, R. Fleischhauer, U. Pika-Hartlaub, T. Malina, N. Mitrovic, and F. Lehmann-Horn. 1997. Role in fast inactivation of the IV/S4-S5 loop of the human muscle Na+ channel probed by cysteine mutagenesis. *J. Physiol.* 505:345–352. http://dx.doi.org/10.1111/j.1469-7793.1997.345bb.x

McPhee, J.C., D.S. Ragsdale, T. Scheuer, and W.A. Catterall. 1998. A critical role for the S4-S5 intracellular loop in domain IV of the sodium channel alpha-subunit in fast inactivation. *J. Biol. Chem.* 273:1121–1129. http://dx.doi.org/10.1074/jbc.273.2.1121

Muroi, Y., M. Arcisio-Miranda, S. Chowdhury, and B. Chanda. 2010. Molecular determinants of coupling between the domain III voltage sensor and pore of a sodium channel. *Nat. Struct. Mol. Biol.* 17:230–237. http://dx.doi.org/10.1038/nsmb.1749

Richard Benzinger, G., G.S. Tonkovich, and D.A. Hanck. 1999. Augmentation of recovery from inactivation by site-3 Na channel toxins. A single-channel and whole-cell study of persistent currents. *J. Gen. Physiol.* 113:333–346. http://dx.doi.org/10.1085/jgp.113.2.333

Sheets, M.F., J.W. Kyle, R.G. Kallen, and D.A. Hanck. 1999. The Na channel voltage sensor associated with inactivation is localized to the external charged residues of domain IV, S4. *Biophys. J.* 77:747–757. http://dx.doi.org/10.1016/S0006-3495(99)76929-8

Sheets, M.F., J.W. Kyle, and D.A. Hanck. 2000. The role of the putative inactivation lid in sodium channel gating current immobilization. *J. Gen. Physiol.* 115:609–620. http://dx.doi.org/10.1085/jgp.115.5.609

Smith, M.R., and A.L. Goldin. 1997. Interaction between the sodium channel inactivation linker and domain III S4-S5. *Biophys. J.* 73:1885–1895. http://dx.doi.org/10.1016/S0006-3495(97)78219-5

Vandenberg, C.A., and F. Bezanilla. 1991. A sodium channel gating model based on single channel, macroscopic ionic, and gating currents in the squid giant axon. *Biophys. J.* 60:1511–1533. http://dx.doi.org/10.1016/S0006-3495(91)82186-5

Wallace, R.H., D.W. Wang, R. Singh, I.E. Scheffer, A.L. George Jr., H.A. Phillips, K. Saar, A. Reis, E.W. Johnson, G.R. Sutherland, et al. 1998. Febrile seizures and generalized epilepsy associated with a mutation in the Na+-channel beta1 subunit gene SCN1B. *Nat. Genet.* 19:366–370. http://dx.doi.org/10.1038/448

Wang, D.W., K. Yazawa, A.L. George Jr., and P.B. Bennett. 1996. Characterization of human cardiac Na+ channel mutations in the congenital long QT syndrome. *Proc. Natl. Acad. Sci. USA.* 93:13200–13205. http://dx.doi.org/10.1073/pnas.93.23.13200

Wang, Q., J. Shen, Z. Li, K. Timothy, G.M. Vincent, S.G. Priori, P.J. Schwartz, and M.T. Keating. 1995a. Cardiac sodium channel mutations in patients with long QT syndrome, an inherited cardiac arrhythmia. *Hum. Mol. Genet.* 4:1603–1607. http://dx.doi.org/10.1093/hmg/4.9.1603

Wang, Q., J. Shen, I. Splawski, D. Atkinson, Z. Li, J.L. Robinson, A.J. Moss, J.A. Towbin, and M.T. Keating. 1995b. SCN5A mutations associated with an inherited cardiac arrhythmia, long QT syndrome. *Cell.* 80:805–811. http://dx.doi.org/10.1016/0092-8674(95)90359-3

West, J.W., D.E. Patton, T. Scheuer, Y. Wang, A.L. Goldin, and W.A. Catterall. 1992. A cluster of hydrophobic amino acid residues required for fast Na(+)-channel inactivation. *Proc. Natl. Acad. Sci. USA.* 89:10910–10914. http://dx.doi.org/10.1073/pnas.89.22.10910

Yang, N., and R. Horn. 1995. Evidence for voltage-dependent S4 movement in sodium channels. *Neuron.* 15:213–218. http://dx.doi.org/10.1016/0896-6273(95)90078-0